

## NEW SUNS IN THE COSMOS III: MULTIFRACTAL SIGNATURE ANALYSIS

D. B. DE FREITAS, M. M. F. NEPOMUCENO, P. R. V. DE MORAES JUNIOR, C. E. F. LOPES, M. L. DAS CHAGAS, J. P. BRAVO, A. D. COSTA, B. L. CANTO MARTINS, J. R. DE MEDEIROS

Departamento de Física, Universidade Federal do Rio Grande do Norte, 59072-970 Natal, RN, Brazil

I. C. LEÃO

European Southern Observatory, Karl-Schwarzschild-Str. 2, 85748 Garching, Germany

### ABSTRACT

In present paper, we investigate the multifractality signatures in hourly time series extracted from CoRoT spacecraft database. Our analysis is intended to highlight the possibility that astrophysical time series can be members of a particular class of complex and dynamic processes which require several photometric variability diagnostics to characterize their structural and topological properties. To achieve this goal, we search for contributions due to nonlinear temporal correlation and effects caused by heavier tails than the Gaussian distribution, using a detrending moving average algorithm for one-dimensional multifractal signals (MFDMA). We observe that the correlation structure is the main source of multifractality, while heavy-tailed distribution plays a minor role in generating the multifractal effects. Our work also reveals that rotation period of stars is inherently scaled by degree of multifractality. As a result, analyzing the multifractal degree of referred series, we uncover an evolution of multifractality from shorter to larger periods.

*Keywords:* stars: solar-type — stars: rotation — Sun: rotation — methods: data analysis

### 1. INTRODUCTION

In different areas of knowledge, many phenomena have been demonstrated to be governed by nonlinear dissipative systems and manifest (multi)fractal and complex structures in one-dimensional signals and images (Hurst, Black & Simaika 1965; Feder 1988; Komm 1995; Ivanov et al. 1999; Chappell & Scalo 2001; Norouzzadeha, Dullaert & Rahmani 2007; de Freitas et al. 2013a). In particular, these phenomena exhibit linear or nonlinear behavior depending on how the output energy is related to the input energy of the system (Mandelbrot & Wallis 1969a,b,c; Aschwanden & Parnell 2002; Aschwanden 2011). This transitional process is associated with entities that interact in a complex manner that requires (i) a continuous energy input source and (ii) a nonlinear dissipative system. In stellar physics, the mechanisms of the solar dynamo operation can be supported by a dominance of large or small fluctuations in the total energy emitted by solar indicators, such as flares and sunspots (Movahed et al. 2006; Sen 2007; de Freitas & De Medeiros 2009).

Recently, de Freitas et al. (2013b) discussed the statistical and fractal properties of CoRoT time series due to cyclic behavior attributed to magnetic activity on the stellar photosphere, particularly rotational modulation (Baglin 2006). The importance of astrophysical time series analyses, which typically exhibit non-stationary and nonlinear dynamics, has been recognized in the area of complex systems analysis and self-organized criticality (SOC) (Watari 1996; Aschwanden & Parnell 2002). Several features of these approaches have been adopted to detect the spatiotemporal dynamical behavior of astrophysical phenomena. An important approach based on measuring the smoothness of a fractal time series and thereby characterizing signals is the traditional rescale range analysis ( $R/S$ ) method based on a power-law with slope  $H$ , i.e., the Hurst exponent (Hurst 1951; Hurst, Black & Simaika 1965).  $R/S$  analysis is a statistical technique used for detecting persistence, randomness, or mean reversion in time series through the exponent  $H$  statistically known as an index of long-memory process. Using this method, de Freitas et al. (2013b) demonstrated that different centers of rotation due to modulation affect the slope  $H$  on different timescales, corresponding to sub-harmonics of rotation period of each star. These centers of rotation can be associated to chaotic motions temporally aperiodic (neither random, nor periodic) due to a fractal hierarchic structure (Suyal, Prasad & Singh 2009; de Freitas

et al. 2013b).

The variation in the Hurst exponent  $H$  in different time windows can be used to quantify dynamic changes in the features of a time series. As an example, lower  $H$  values characterize the portions of the signal with lower complexity. In contrast, higher values reveal strong interactions in the time series dynamics. This behavior clearly complements a wide range of methods that are routinely used in astrophysics, such as Lomb-Scargle periodograms, autocorrelation functions and Gaussian processes (Lomb 1976; Scargle 1982). Similarly, different levels of complexity can be associated with an anti-persistence/persistence (i.e., whether fractional Brownian motion is obeyed) processes extracted by a fractal spectral analysis in terms of the local Hurst exponent. As noted by de Freitas et al. (2013b), the exponent  $H$  can indicate a quantification of variability in relatively brief and noisy time series.

In this sense, astrophysical time series can be classified as members of a class of physical ensembles that involve long-range interactions (complex fluctuations), long-range microscopic memories (e.g., non-Markovian stochastic processes), or multifractal structures. In this context, time-domain astrophysics cannot be treated using traditional statistical analysis methods for a wide range of problems (Feigelson & Babu 2012). Several sources of multifractality are not captured by conventional measures, such as Fourier and wavelet analysis (Bravo et al. 2011). For instance, a rotational signature has a scale-invariant structure, i.e., it does not change if scales of length of the time windows are multiplied by a factor. Mathematically, a time series  $x(t)$  is scale-free when  $x(ct) = c^H x(t)$ , i.e., it does not obey the homogeneity property and it is described by a power law rather than a Gaussian distribution, which is typical in monofractal systems (Aschwaden 2011; Ihlen 2012). Signals with structures that are independent of time and space are known as monofractals and are defined by a single power law exponent, i.e., one unique value for  $H$ . Nonetheless, spatial and temporal variations in scale-invariant structures are most common in astrophysical scenarios. In this case, they are best defined by a  $H$  spectrum, i.e., the Holder spectrum (de Freitas et al. 2013b).

Some authors (e.g., Suyal, Prasad & Singh 2009; de Freitas et al. 2013b) have shown that the variations in stellar magnetic activity present a global value of  $H$  greater than 0.5, indicating long-term memory in the time series (Kantelhardt et al. 2002). However, a multifractal time series not only exhibits long-range correlations over different time scales but can also result from heavy tails in the probability distributions even if the data have no memory (Grech & Pamula 1982). In finite datasets, large fluctuations cannot be detected, only small fluctuations. In other words, the multifractal properties of shorter time series reveal a wide variety of fluctuations at different scales, whereas longer time series are corrupted by various effects, such as noise, short-term memory or periodic signals (Grech & Pamula 1982).

de Freitas et al. (2013b) observed fractality traces in the time series of the Sun in its active and quiet phases and in a sample of 14 CoRoT stars with sub- and super-solar rotational periods and 3 stars with period near the solar value (Lanza et al. 2003). It is worth noting that our selected stars present values of  $\log T_{eff}$  (effective temperature) between  $\sim 3.62$  and  $\sim 4.39$  and  $\log g$  (effective gravity) from 2.8 to 4.6 (De Medeiros et al. 2013). These researchers computed the global Hurst exponent for these stars and found a clear correlation between the Hurst exponent and rotational period. This result reveals that the global Hurst exponent can be considered as a powerful classifier for noisy semi-sinusoidal time series. However, the  $R/S$  analysis is considered under the hypothesis that the working sample is monofractal, i.e., characterized by a global singularity exponent. In addition, local scaling exponents can be revealed considering a priori that the sample is intrinsically more complex and dynamic than a monofractal. There are a vast number of methods that have been developed to investigate the behavior and properties of monofractal and multifractal systems. Among them, we can cite classic rescaled range analysis ( $R/S$ ) (Hurst 1951; Hurst, Black & Simaika 1965) and the detrended fluctuation analysis (DFA) (Taqqu et al. 1995) and detrended moving average (DMA) algorithm (Alessio et al. 2002), all of which have been appropriated for fractal time series. The wavelet-based transform module maxima (WTMM) (Muzy et al. 1991, 1994), multifractal detrended fluctuation analysis (MFDFA) (Kantelhardt et al. 2002) and multifractal detrended moving average (MFDMA) (Gu & Zhou 2010) are commonly used for multifractal time series. Independent of the (multi)fractal analysis method applied, the multifractal spectrum is one of most important products used to study complex time series (cf. Gu & Zhou 2010). Previous studies have noted that MFDMA is slightly better than WTMM and MFDFA for the performance and multifractal characterization of time series data (Ruan & Zhou 2011; Zhou 2012).

The main purpose of the present work is to examine the correlation between the multifractality signatures and stellar variability in time series of less than 150 days, a phenomenon that has been investigated in a pioneering study published by de Freitas et al. (2013b). Indeed, we will investigate the behavior of the variability in the same CoRoT sample analyzed by these authors. In this context, we will compare the results of the multifractal analysis for original, shuffled and phase-randomized data and verify whether the processes are affected by strong correlations and nonlinearity, among other features. The remainder of this paper is organized as follows. In the next section, we

describe the methods used in our analysis. In section 3, we provide our results and discuss their implications, and in the last section, we present our final remarks.

## 2. PROCEDURES AND MULTIFRACTAL ANALYSIS

The main feature of multifractals is that the fractal dimension is not the same on all scales. In case of a one-dimensional signal, the fractal dimension can vary from unity to a dot. This property reveals a variability spectrum on a wide range of temporal scales, associated with quasi- or periodic fluctuations and power-law-like correlations due to astrophysical noise. For our particular case, we have chosen an extended version of the detrended moving average (DMA) algorithm, which consists of a multifractal characterization of nonstationary time series (Gu & Zhou 2010). Whereas the DMA method generates the same scaling properties throughout the entire signal indexed by a single global Hurst exponent, the MFDMA details the signal on a wide Hurst exponent spectrum. Thus, the Hurst exponent defined by the DMA method represents the average fractal structure of the entire signal, thus representing the central tendency of the multifractal spectrum (Alessio et al. 2002).

Our sample is composed of time series of the Sun (Virgo/SOHO light curves in two regimes: active and quiet) and 14 obtained from CoRoT spacecraft (all presenting rotational modulation) with  $\log T_{eff}$  varying from 3.6 to 3.8, i.e., from fully convective M stars to the Kraft break (Kraft 1967). The time series examined in our work present a regular dynamics due to rotational modulation in a wide interval of frequencies and irregular dynamics due to astrophysical noise, thus making them suitable candidates for multifractal analysis. We applied the one-dimensional multifractal detrending moving average analysis (MFDMA) according to the procedure summarized in (Gu & Zhou 2010).

In general, a time series is composed by a deterministic function  $p(t, \bar{P})$ , where the vector  $P$  is a Fourier series, and a stochastic term characterized by astrophysical noise (without instrumental bias) given by  $\eta(t)$ . In this sense, a time series  $x(t)$  can be written as

$$x(t) = p(t, \bar{P}) + \eta(t), \quad (1)$$

where  $\eta(t)$  represents the colorful noise associated with the  $1/f^\gamma$ -like one in Carter & Winn (2009). The parameter  $\gamma$  consists of the color index of the noise and is associated with the global Hurst exponent  $H$  by the relation  $\gamma = H \pm 1$ , as noted by Pascual-Granado (2011) and de Freitas et al. (2013b).

In general, all procedures that involve a multifractal background generate three crucial parameters to describe the structural properties of a time series  $x(t)$ : (i) a  $q$ th-order fluctuation function  $F_q(n)$ , (ii) the multifractal scaling exponent  $\tau(q)$  (i.e., the Renyi exponent), and (iii) the multifractal spectrum  $f(\alpha)$ . These parameters are obtained according to the following steps:

- First, the time series is reconstructed as a sequence of cumulative sums given by

$$y(t) = \sum_{i=1}^t x(i), \quad t = 1, 2, \dots, N, \quad (2)$$

where  $N$  is the length of the signal.

- Second, the moving average function  $\tilde{y}(t)$  of Eq. (2) is calculated in a moving window:

$$\tilde{y}(t) = \frac{1}{n} \sum_{k=-\lfloor (n-1)\theta \rfloor}^{\lceil (n-1)(1-\theta) \rceil} y(t-k), \quad (3)$$

where  $n$  is the window size,  $\lceil (\cdot) \rceil$  is the largest integer not larger than argument  $(\cdot)$ ,  $\lfloor (\cdot) \rfloor$  is the smallest integer not smaller than argument  $(\cdot)$ , and  $\theta$  is the position index with values between 0 and 1. In present work,  $\theta$  was adopted as 0, referring to the backward moving average, i.e.,  $\tilde{y}(t)$  is calculated over all the past  $n-1$  data of the time series (for more details, see Gu & Zhou 2010);

- Third, the trend is removed from the reconstructed time series  $y(t)$  using the function  $\tilde{y}(t)$  and the residual sequence  $\epsilon(t)$  is obtained:

$$\epsilon(i) = y(i) - \tilde{y}(i), \quad n - \lfloor (n-1)\theta \rfloor \leq i \leq N - \lfloor (n-1)\theta \rfloor \quad (4)$$

where, this residual time series  $\epsilon(i)$  is subdivided into  $N_n$  disjoint segments with the same size  $n$  given by  $\lfloor N/n - 1 \rfloor$ . In this sense, the residual sequence  $\epsilon(t)$  for each segment is denoted by  $\epsilon_\nu$ , where  $\epsilon_\nu(i) = \epsilon(l+1)$  for  $1 \leq i \leq n$  and  $l = (\nu-1)n$ ;

- Fourth, we calculate the root-mean-square (rms) function  $F_\nu(n)$  for a segment size  $n$ ,

$$F_\nu(n) = \left\{ \frac{1}{n} \sum_{i=1}^n \epsilon_\nu^2(i) \right\}^{\frac{1}{2}}. \quad (5)$$

- Fifth, the generating function of  $F_q(n)$  is determined as

$$F_q(n) = \left\{ \frac{1}{N_n} \sum_{\nu=1}^{N_n} F_\nu^2(n) \right\}^{\frac{1}{q}}, \quad (6)$$

for all  $q \neq 0$  and for  $q = 0$ ; hence,

$$F_q(n) = \exp \left\{ \frac{1}{2N_n} \sum_{\nu=1}^{N_n} \ln[F_\nu^2(n)] \right\}, \quad (7)$$

where the scaling behavior of  $F_q(n)$  follows a power-law type given by  $F_q(n) \sim n^{h(q)}$  and  $h(q)$  represents the local Hurst or Holder exponent.

- Sixth, knowing  $h(q)$ , we can easily derive  $\tau(q)$  using

$$\tau(q) = qh(q) - 1; \quad (8)$$

- Finally, we obtain the Holder exponent  $\alpha(q)$  and the multifractal spectrum  $f(\alpha)$ , which is related to  $\tau(q)$  via a Legendre transform:

$$\alpha(q) = \frac{d\tau(q)}{dq}, \quad (9)$$

where the multifractal spectrum is defined as

$$f(\alpha) = q\alpha - \tau(q). \quad (10)$$

It is important to stress that in present study, the backward MFDMA algorithm ( $\theta = 0$ ) gives us a best computation accuracy of the exponent  $\tau(q)$ , as well as mentioned by [Gu & Zhou \(2010\)](#).

As noted by [Teslesca & Lapenna \(2006\)](#), the multifractal spectrum provides detailed information about the relative importance of several types of fractal exponents present in the signal. To quantitatively characterize the multifractal spectrum, we investigate the behavior of two features extracted from the  $[\alpha, f(\alpha)]$  plot: the width of  $\alpha$ , which indicates the degree of multifractality, and the asymmetry in the shape of  $\alpha$ . The width of  $\alpha$  is defined as  $\Delta\alpha = \alpha_{max} - \alpha_{min}$ ; we measured this width by extrapolating the fitted curve to zero, i.e., by determining the roots of a 4th-order polynomial. The parameter  $\Delta\alpha$  can also be understood as a measure of the multifractal diversity or complexity of signal. For instance, larger values of  $\Delta\alpha$  indicate a richer and more complex structure, whereas smaller values indicate the monofractal limit. The asymmetry in the shape of  $\alpha$  is defined as  $A = \frac{\alpha_{max} - \alpha_0}{\alpha_0 - \alpha_{min}}$ , where  $\alpha_0$  is the value of  $\alpha$  when  $f(\alpha)$  assumes its maximum value. According to the latter relation, the asymmetry  $A$  presents three shapes: asymmetry to the right-skewed ( $A > 1$ ), left-skewed ( $0 < A < 1$ ) or symmetric ( $A = 1$ ). As noted by [Sen \(2007\)](#) and [Ihlen \(2012\)](#), an asymmetry to a long left tail indicates a multifractal structure that is insensitive to local fluctuations with small magnitudes, whereas a long right tail refers to a structure that is insensitive to local fluctuations with large magnitudes. In the stellar rotation scenario, these fluctuations can be associated with semi-sinusoidal signatures and background noise ([De Medeiros et al. 2013](#); [de Freitas et al. 2013b](#)).

In addition to the original data treatment, we apply the MFDMA in two other procedures. These two methods, *shuffling* and *phase randomization*, are used to verify the origin of the multifractality. Shuffling a time series destroys the long-range temporal correlation for small and large fluctuations and preserves the distribution of the data. In other words, the distribution function of the original data remains the same but without memory, i.e.,  $\alpha_0$  is shifted to  $\sim 0.5$ . The origin of multifractality can also be due to fat-tailed probability distributions present in the original time series. For this case, the non-Gaussian effects can be weakened by creating phase-randomized surrogates. In this context, the procedure preserves the amplitudes of the Fourier transform and the linear properties of the original series but randomizes the Fourier phases while eliminating nonlinear effects ([Norouzzadeha, Dullaert & Rahmani 2007](#)). These procedures are used to study the degree of complexity of time series to distinguish different sources of multifractality in the time series.

Each source can be investigated by using the Holder exponent  $h(q)$ . Thus, if the shuffled signal only presents long-range correlations, we should find that  $h_{shuf}(q) = 0.5$ . However, if the source of multifractality is due to a heavy-tailed distributions obtained by the surrogate method, the values of  $h_{sur}(q)$  will be independent of  $q$ . An alternative method to assess the behavior of multifractality is to compare the multifractal scaling exponent  $\tau(q)$  for the original, shuffled and surrogate data. Differences between these two scaling exponents and the original exponent reveal the presence of long-range correlations and/or heavy-tailed distributions. Using Eq. (8), this comparison can be shown in a plot, which presents the following relations:

$$\tau(q) - \tau_{shuf}(q) = q[h(q) - h_{shuf}(q)] = qh_{corr}(q) \quad (11)$$

and

$$\tau(q) - \tau_{sur}(q) = q[h(q) - h_{sur}(q)] = qh_{tail}(q), \quad (12)$$

where we should find that  $h(q) = h_{shuf}(q)$  and thus that  $h_{corr}(q) = 0$  if the multifractality is due solely to the heaviness of the distribution. The multifractality indicates the presence of long-range correlations if  $h_{corr}(q) \neq 0$ . However, if the source is due solely to correlations, we will find that  $h_{shuf}(q) = 0.5$ . If both sources are present,  $h_{corr}(q)$  and  $h_{tail}(q)$  will depend on  $q$ .

### 3. RESULTS AND DISCUSSION

The results described by [de Freitas et al. \(2013b\)](#) suggest a correlation between the Hurst exponent and rotation period (including the Sun), but the source of this correlation was not discussed. In the present paper, we revisit the same sample using a multifractal approach that highlights different features that occur on small and large time scales, whereas the approach used by [de Freitas et al. \(2013b\)](#) restricts the analysis to global behavior characterized by a single “mean” exponent. All original data present in our work are associated with a nonlinear  $\tau(q)$  plot indicated by a crossover at  $q = 0$  (see Figs. 1 to 4, left-bottom panels). As reported by [Movahed et al. \(2006\)](#), the presence of a crossover in  $[q - \tau(q)] - plot$ , i.e., different slopes for  $q < 0$  and  $q > 0$ , emphasizes that the multifractality in the time series is extremely strong.

The top panels of Figs. 1 through 4 illustrate the multifractal fluctuation function  $F_q(n)$  obtained from the MFDMA for an extract of our stellar sample (including the Sun), where each curve corresponds to different fixed values of  $q = -5, \dots, 0, \dots, 5$  in steps of 0.2. The values for the scale parameter  $n$  were varied from 10 to  $N/10$  ([Chappell & Scalo 2001](#); [Gu & Zhou 2010](#)). In the top-left figures, the top, middle and bottom bold lines correspond to  $q = 5$ ,  $q = 0$  and  $q = -5$ , respectively; the black lines represent the shuffled data, and the red lines indicate the original data. The different slopes  $h(q)$  of each curve indicate that the small and large fluctuations scale differently. The multifractal scaling exponent  $\tau(q)$  of the original, shuffled and surrogate time series are compared in the bottom-left panel. The multifractal spectra  $f(\alpha)$  of the original, shuffled and surrogate time series are shown in the bottom-right panel, in which the solid curves represent the best 4th-order fit.

As shown by figures of the active Sun and the best candidate (CoRoT ID 105693572) for a new Sun (figs. 1 (left panel) and 2 (right panel), respectively), the stars differ from the perspective of a multifractal analysis. As quoted by [de Freitas et al. \(2013b\)](#), the “New Suns” candidates were selected by the best values for the triplet (Hurst exponent, effective temperature and rotation period), where the star CoRoT ID 105693572 is the best candidate by presenting the values of this triplet most similar to the Sun. In general, some stellar indicators, such as flares and smallest spots, are not detected by instruments because the flux from a light source is proportional to the inverse square of the distance, limiting the instrumental sensitivity of the detectors (for more details, see [Aschwaden 2011](#)). Furthermore, this behavior can also be influenced by the cycle phase of the star.

#### 3.1. Results based on resampled data

As mentioned the previous Section, two different kinds of multifractality can be identified in a time series. One of them destroys the long range correlation by the shuffling procedure, where if the multifractality only is due to this type of correlation, we should find  $h_{shuf}(q) = 0.5$ . These resampled data are shown by green cycles in Figs. 1 through 4. As illustrated in Figs. 1 and 2, the active Sun is more “polluted” by correlated noise on different scales than the **referred** star CoRoT ID 105693572 using the values of  $\alpha_0$  of the multifractal spectrum from the shuffled time series as the distinguishing parameter. As discussed in the next section, a white-noise-like time series (shuffled one) has a time-independent structure with  $\alpha_0 \sim 0.5$ , as shown by the vast majority of our sample. In contrast, both the active and quiet Sun present values of  $\alpha_0 \sim 1$ , indicating that the noise is  $1/f^\gamma$ -like, i.e., a time-correlated noise ([Carter & Winn 2009](#); [Aschwaden 2011](#)).



After shuffling, the time series exhibit an even smaller degree of multifractality than the original one for all stars, except for the quiet Sun and CoRoT ID 105945509. This result can be emphasized by the multifractal spectra, for which  $\Delta\alpha - \Delta\alpha_{shuf} > 0$ . Therefore, as described below, this analysis is insufficient for explaining the source of this behavior. In this case, the behavior of  $\tau(q)$  must be verified using the relations 11 and 12. As illustrated by Figs. 5 and 6, there is a dependence of  $h_{corr}(q)$  on  $q$ , which is clearest for  $q < 0$ , where a long right tail occurs, as shown in the lower panels of Figs. 1 through 4.

### 3.2. Results based on phase randomized data

As the shuffling procedure does not remove the multifractality due to a heaviness of distribution, we apply the surrogate method to clarify the contribution due to the phase randomization of discrete Fourier transform coefficients of time series. In contrast to the results found in previous subsection, for  $q > 0$  the dependence on  $q$  can be neglected for the surrogate data in all stellar samples, including the Sun, as shown in Figs. 5 and 6. In fact, the absolute values of  $h_{corr}(q)$  in both domains ( $q < 0$  and  $q > 0$ ) are typically greater than  $h_{tail}(q)$ , thus implying that the multifractality due to heaviness is weaker than the multifractality due to long-range correlations. According to the central limit theorem, the superposition of many small and independent effects with finite statistical moments leads to a Gaussian distribution. This means that the small deviations found between the surrogate and original data reduce to the typical condition of the random variables of a system being independent with an approximately linear behavior (Hilhorst 2009). The results suggest that our sample does not contain important phase correlations that are canceled in the surrogate time series by randomization of the Fourier phases. Thus, the observed multifractality is related to the long-range correlation generated by rotational modulation, except for the quiet Sun.

### 3.3. The degree of multifractality and asymmetry

Another class of results is associated with the correlation between the stellar parameters and the parameters extracted from our method. The top panel of Fig. 7 provides the values for the degree of multifractality ( $\Delta\alpha$ ) based on the multifractal analysis as a function of the rotation period. The solid line denotes the linear regression obtained through a similar adjustment as derived by de Freitas et al. (2013b). In this context, the period is related to not only a single exponent but also the multifractal diversity spectrum. In contrast, the  $\Delta\alpha$ – $A$  correlation indicates that different domains can be separated. The values of the parameters extracted from multifractal analysis are summarized in Table 8. This result demonstrates that the transition region between left and right asymmetry, indicated by the horizontal line (see bottom panel in Fig. 7), can serve as a dividing line to distinguish stars in the active and quiet phases. In future works, this procedure can be used as a method for discriminating “blind” datasets. Besides, this figure reveals the lack of a clear correlation between the asymmetry parameter and the degree of multifractality.

Finally, in contrast to de Freitas et al. (2013b), these behaviors demonstrate that a single exponent is not sufficient to describe the complexity of a stellar time series. It is important to emphasize that there are several alternative methods to deal with the complexity of time series, including time-domain, wavelets and spectrum-based techniques. In general, these methods are based into three main categories, namely *fractality*, *nonlinear dynamics* and *entropy*, which can broaden the range of procedures and tools for handling the problems mentioned in present work. We focus on fractality methods by analysing the geometric properties of a set of data. A literature review of most important methods for analysing time series can be found in Tang et al. (2015).

### 3.4. Interpretation of the physical origin

We verified for possible correlations between our multifractal indexes ( $\Delta\alpha$  and  $A$ ) and effective temperature and surface gravity extracted by Sarro et al. (2013). This analysis indicates that these basic stellar properties are weakly correlated with multifractal indexes, exhibiting absolute values of the Spearman’s correlation coefficient  $r < 0.1$  (Press et al. 2007). Likewise, we also investigate whether this correlation could be caused by another physical source linked to star’s brightness variations. Following Karoff et al. (2013), there are, at least, two approaches of the physical processes responsible for distinct features in solar frequency spectrum. Generally speaking, the manifestation of the different physical processes in time series as a function of frequency, such as granulation, faculae or oscillation, is prone to the cadence of data as reported by Karoff et al. (2013) (see Table 2, here adopted).

In general, as pointed by Del Moro (2004), the granular lifetime distributions follow a decaying exponential law, indicating that the signature due to granulation occurs at frequencies higher than  $1000\mu\text{Hz}$  ( $\leq 17$  min). In agreement with the long-cadence data ( $\sim 1\text{h}$ ) adopted here, this signature can be neglected in our study. At the same time, there is another type of stellar granulation that appears at lower frequencies denoted flicker noise. As reported by Bastien et al. (2013), flickers are revealed on timescales shorter than 8 hours (in particular,  $F_8$ ) and are widely used as a proxy

for the surface gravity. In fact, in the present literature, flicker is considered only calibrated to surface gravity. Our results show that there is no evidence of a correlation between the degree of multifractality and the surface gravity and, therefore, we could infer that the effects due to flicker noise can be neglected. However, as shown in Fig. 8, a more depth analysis reveals that  $\Delta\alpha$  and  $F_8$  are correlated with Spearmans coefficient of -0.48. The present study applies the same procedure used by Bastien et al. (2013) and Kipping et al. (2014) to compute the variability in photometric brightness due to  $F_8$ . Thus, our multifractal analysis suggests that the physical origin of the correlation between the rotation period and the degree of multifractality can be due to rotational modulation from long-lived spots (Radick et al. 1998; Lanza, Rodono & Pagano 2004). On the other hand, our results point out that the flicker is a very good candidate for explaining the changes in the multifractal index.

In addition, the CoRoT time series typically have a cadence shorter than a dozen of minutes (de Freitas et al. 2013b), allowing us to measure different kind of noisy sources, in general, the photon noise (Mathur et al. 2014). However, a complete investigation about the different individual contribution of these sources is out of scope of present paper.

#### 4. FINAL REMARKS

The multifractal properties of our stellar sample have been investigated in this work through the MFDMA method, which was developed to quantify the long-range correlations of non-stationary time series by using a detrending moving average analysis. Applying this method, we demonstrated that hourly time series of a CoRoT stellar sample are characterized by strong long-range correlations due to rotational modulation. This result suggests that our sample exhibits the features that can be invoked in terms of multifractality approaches. The main insight and contribution of our work is to estimate the different levels of multifractality present according to fluctuations arising from stellar variability.

As shown in Figs. 1 through 4, the long left tails are related to the dominant noise amplitude, whereas the long right tails are associated with the dominance of the rotational modulation amplitude. Furthermore, these results indicate that the variability due to rotational modulation is even more complex and dynamic than is indicated by classical statistical methods, such as Fourier analysis and the autocorrelation function.

The analysis of the behavior of the rotation period as a function of the degree of multifractality suggests that the rotation period of stars is inherently scaled by a dynamical change from homogeneity toward heterogeneity, reciprocally, from shorter to larger periods, as emphasized by the growth in multifractality shown in Fig. 7 (see the top panel). This behavior can be related to strong magnetic activity, thus indicating that the multifractal degree is a suitable activity indicator. The method used by de Freitas et al. (2013b) derived a single relation that was in good agreement with the results presented here. Nevertheless, our results highlight that the multifractal analysis has led to a better understanding of how such deterministic and stochastic characteristics are regulated hierarchically.

Another result, but one that requires further studies, is related to the asymmetry of the multifractal spectrum. If this asymmetry is confirmed, the transition region between left and right asymmetries could be used to discriminate between stars in the active and quiet phases. If this hypothesis is true, our work could lead us to assume that each CoRoT star is in the active phase. However, more realistic models and methods must be developed to understand the behavior of astrophysical noise and the fluctuations due to the starspot lifetime. Finally, our multifractal approach can be a useful tool for understanding the dynamical mechanisms that control stellar magnetic activity.

Research activities of the Astronomy Observational Board of the Federal University of Rio Grande do Norte are supported by continuous grants from CNPq and FAPERN brazilian agencies. We also acknowledge financial support from INCT INEspaço/CNPq/MCT. MLC, JPB and ADC acknowledge a CAPES/PNPD fellowship. MMFN and PRVM acknowledge graduate fellowships from CAPES. DBF also acknowledges financial support by the Brazilian agency CNPq (Grant No. 306007/2015-0).

#### REFERENCES

- |   |  |
|---|--|
| <p>Alessio, E., Carbone, A., Castelli, G., &amp; Frappietro, V. 2002, <i>Eur. Phys. J.</i>, 27, 197</p> <p>Ashwanden, M. J., &amp; Parnell, C. E. 2002, <i>Astrophys. J.</i>, 572, 1048</p> <p>Ashwanden, M. J. 2011, <i>Self-Organized Criticality in Astrophysics. The Statistics of Nonlinear Processes in the Universe</i>, Springer-Praxis: New York</p> | <p>Baglin, A. 2006, in <i>ESA Special Publication</i>, Vol. 1306, ed. M. Fridlund, A. Baglin, J. Lochard, &amp; L. Conroy, 111</p> <p>Bastien, F. A., Stassun, K. G., Basri, G., &amp; Pepper, J. 2013, <i>Nature</i>, 500, 427</p> <p>Bravo, J. P., Roque, S., Estrela, R., Leão, I. C., &amp; De Medeiros, J. R. 2014, <i>A&amp;A</i>, 568, 34</p> <p>Carter, J. A., &amp; Winn, J. N. 2009, <i>ApJ</i>, 704, 51</p> <p>Chappell, D., &amp; Scalo, J., 2001, <i>ApJ</i>, 551, 712.</p> |
|---|--|

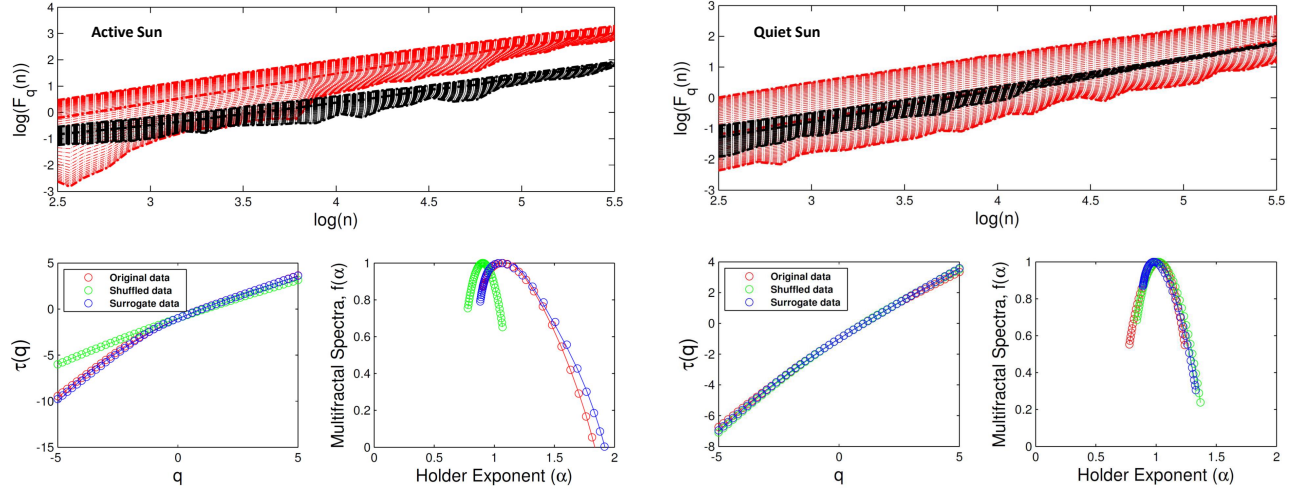


**Figure 1.** The multifractal fluctuation function  $F_q(n)$  obtained from MFDMA for active (left panels) and quiet (right panels) Sun. Each curve corresponds to different fixed values of  $q = -5, \dots, 5$  from top to bottom, while top bold, middle bold lines and bottom bold line correspond to  $q = 5$ ,  $q = 0$  and  $q = -5$ , respectively, where black lines are shuffled data and red lines are original data (*top*). Comparison of the multifractal scaling exponent  $\tau(q)$  of the original (red), shuffled (green) and surrogate (blue) time series (*left – bottom*). Multifractal spectrum  $f(\alpha)$  of the the original (red), shuffled (green) and surrogate (blue) time series. The solid curves represent the best 4th order fit (*right – bottom*).

- De Medeiros, J. R., Lopes, C. E. F., Leão, I. C., et al. 2013, A&A, 555, 63
- de Freitas, D. B., & De Medeiros, J. R. 2009, Europhys. Lett, 88, 19001
- de Freitas, D. B., França, G. S., Scherrer, T. M., Vilar, C. S., & Silva, R. 2013a, Europhys. Lett., 102, 39001
- de Freitas, D. B., Leão, I. C., J. R., Lopes, C. E. F., De Medeiros, J. R., et al. 2013b, ApJL, 773, L18
- Feder, J. 1988, Fractals, Plenum Press, New York
- Feigelson, E. D., & Jogesh Babu, G. 2012, Modern Statistical Methods for Astronomy, Cambridge University Press (Cambridge, UK)
- Gu, G.-F., & Zhou, W.-X. 2010, Phys. Rev. E, 82, 011136
- Grech, D., & Pamula, G. 2008, Physica A, 387, 4299
- Hilhorst, H. J. 2009, Brazilian Journal of Physics, 39, 2
- Hurst, H. E. 1951, Trans. Am. Soc. Civ. Eng., 116, 770
- Hurst, H. E. & Black, R. P., & Simaika, Y. M. 1965, Long-term storage: an experimental study, Constable, London
- Ihlen, E. A. F. 2012, Front. Physiology 3, 141
- Ivanov, P. Ch., Amaral, L. A. N., Goldberger, A. L., et al. 1999, Nature, 399, 461
- Kipping, D. M., Bastien, F. A., Stassun, K. G., Chaplin, W. J., Huber, D. & Buchhave, L. A. 2014, ApJL, 785, 32
- Kraft, R. P. 1967, ApJ, 150, 551
- Kantelhardt, J.W., Zschiegner, S.A., Koscielny-Bunde, E., Havlin, S., Bunde, S. A., & Stanley, H. E. 2002, Physica A, 316, 87
- Karoff, C., Campante, T. L., Ballot, J., Kallinger, T., Gruberbauer, M., et al. 2013, ApJ, 767, 34
- Komm, R. W. 1965, Solar Phys., 156, 17
- Lanza, A. F., Rodono, M., Pagano, I., et al. 2003, A&A, 403, 1135
- Lanza, A. F., Rodono, M., Pagano, I. 2003, A&A, 425, 707
- Lomb, N. R. 1976, Ap&SS, 39, 447
- Del Moro, D. 2004, A&A, 428, 1007
- Mathur, S., Garcia, R. A., Ballot, J., Ceillier, T., Salabert, D., et al. 2014, A&A, 562, 124
- Movahed, M.S., Jafari, G.R., Ghasemi, F., Rahvar, S., & Reza, M. R. T. 2006. Stat. Mech., 02003
- Mandelbrot, B., & Wallis, J. R. 1969a, Water Resour. Res., 5, 521
- Mandelbrot, B., & Wallis, J. R. 1969b, Water Resour. Res., 5, 967
- Mandelbrot, B., & Wallis, J. R. 1969b, Water Resour. Res., 5, 967
- Muzy, J.-F., Bacry, E., & Arneodo, A. 1994, Phys. Rev. Lett. 67, 3515
- Muzy, J.-F., Bacry, E., & Arneodo, A. 1994, Int. J. Bifurc. Chaos, 4, 245
- Norouzzadeha, P., Dullaertc, W., & Rahmani, B. 2007, Physica A, 380, 333
- Press, W. H., Saul A. T., William T. V., & Brian P. F. 2007, Numerical Recipes in C: The Art of Scientific Computing, Third Edition, Cambridge University Press.
- Radick, R. R., Lockwood, G. W., Skiff, B. A., & Baliunas, S. L. 1998, ApJSS, 118, 239
- Ruan, Y.-P., & Zhou, W.-X. 2011, Physica A, 390, 3512
- Sarro, L. M., Debosscher, J., Neiner, C., et al. 2013, A&A, 550, 120
- Scargle, J. D. 1982, ApJ, 263, 835
- Sen, A. K. 2007, Solar Phys, 241, 67
- Suyal, V., Prasad, A., & Singh, H. P. 2009, Solar Phys., 260, 441
- Pascual-Granado, J. 2011, Highlights of Spanish Astrophysics VI, Proceedings of the IX Scientific Meeting of the Spanish Astronomical Society (SEA), held in Madrid, September 13 - 17, 2010, Eds.: M. R. Zapatero Osorio, J. Gorgas, J. Maz Apellniz, J. R. Pardo, and A. Gil de Paz., p. 744
- Tang, L., Lv, H., Yang, F., & Yu, L. 2015, Chaos, Solitons & Fractals, 81, 117
- Telesca, L., & Lapenna V. 2006, Tecnophys., 423, 115
- Taqqu, M., Teverovsky, V., & Willinger, W. 1995, Fractals, 3, 785
- Watari, S. 1996. Solar Phys, 163, 371
- Zhou, W. -X. 2012, Chaos, Solitons & Fractals, 45, 147



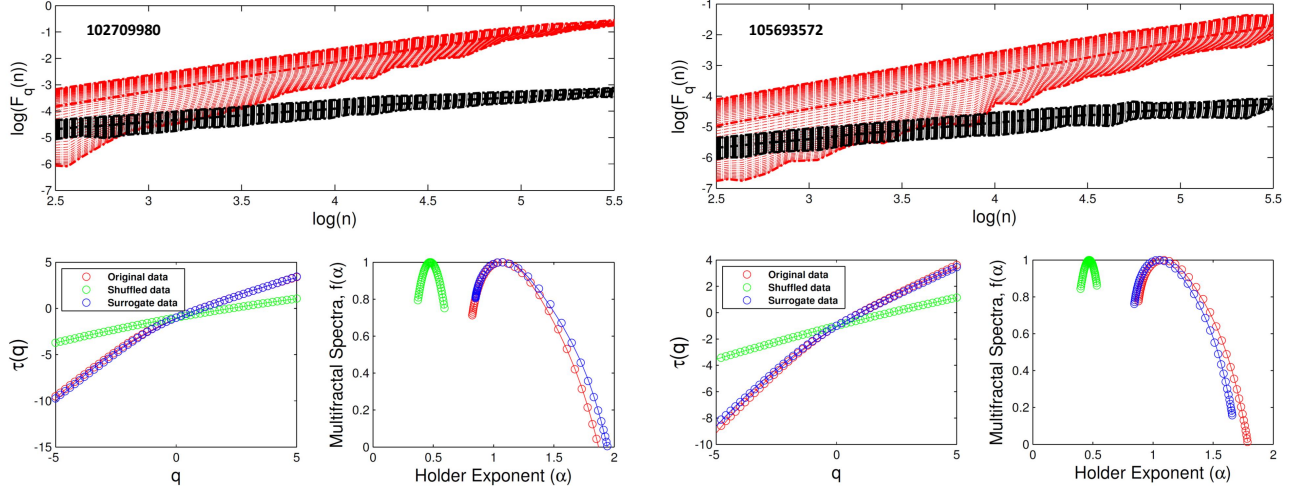


**Figure 2.** Same procedure proposed in figure 1 for the New Suns sample: CoRoT ID 102709980 (left panel) and 105693572 (right panel). As cited by [de Freitas et al. \(2013b\)](#), CoRoTID 105693572 is the best candidate for New Sun.

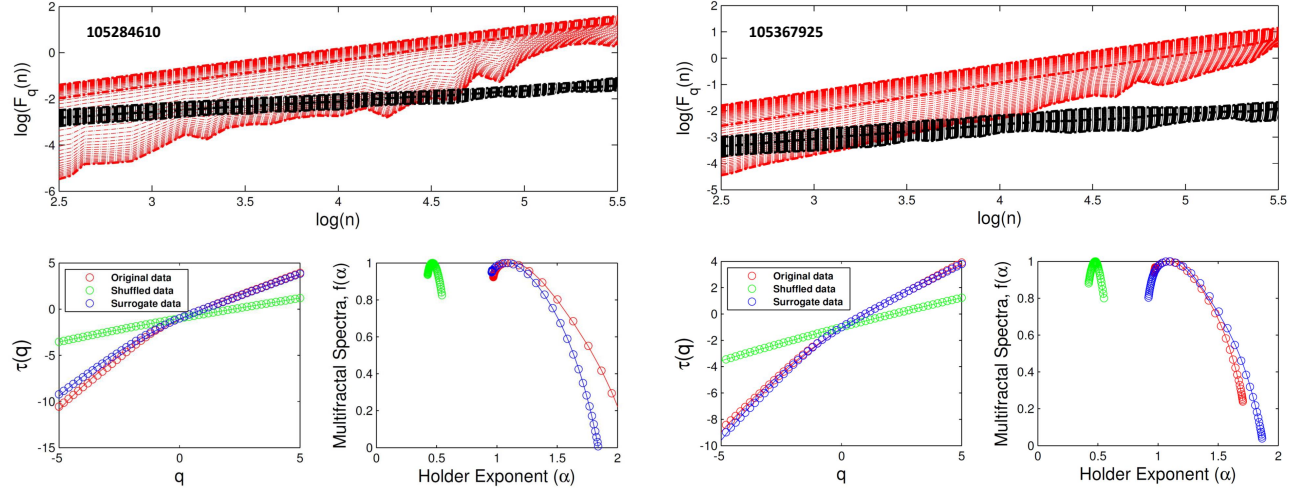


**Figure 3.** Same procedure proposed in figure 1 for the super-solar sample named by CoRoT ID 105284610 (left panel) and 105367925 (right panel).

**Table 1.** Rotation period of our stellar sample and the results of the multifractal analysis.

Star	Broadness ( $\Delta\alpha$ )	Skewness ( $A$ )	$\alpha_0$	logPer (days)	$\delta Per$ (days)
New Sun candidates as Compared with the Sun					
Active Sun	1.18	1.85	1.07	1.52	0.4
Quiet Sun	0.67	0.89	1.02	1.44	0.3
ID 100746852	1.09	1.61	1.08	1.38	0.3
ID 102709980	1.22	1.88	1.07	1.33	0.1
ID 105693572	1.09	1.79	1.09	1.45	0.5
Comparison Stars					
Super-Solar Sample					

Table 1 continued on next page

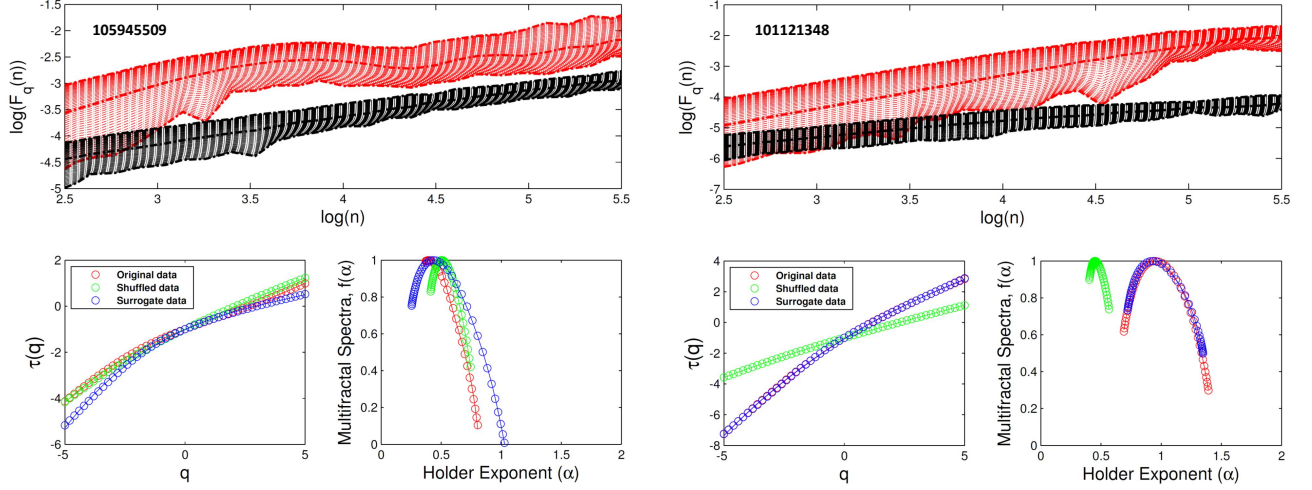


**Figure 4.** Same procedure proposed in figure 1 for the sub-solar sample named by CoRoT ID 105945509 (left panel) and 101121348 (right panel).

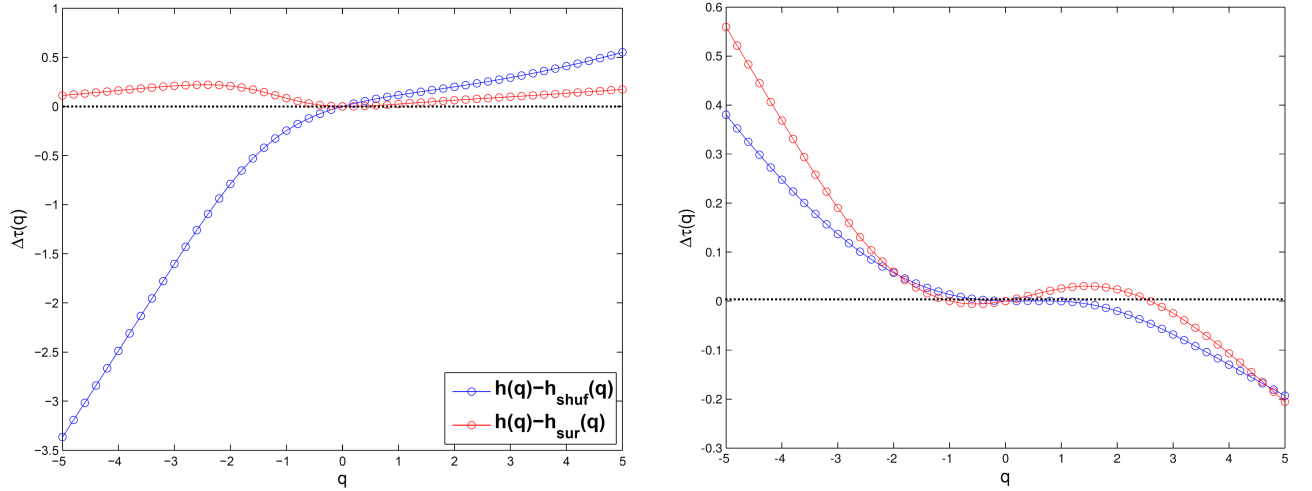


**Figure 5.** Deviations  $\Delta\tau(q)$  as a function of  $q$  between the fluctuation functions with the active (left panel) and quiet (right panel) Sun original data, respectively, due to long-range correlations and broadness of probability distribution.

Table 1 (*continued*)

Star	Broadness ( $\Delta\alpha$ )	Skewness ( $A$ )	$\alpha_0$	logPer (days)	$\delta Per$ (days)
ID 105085209	1.23	2.04	1.12	1.60	0.9
ID 105284610	1.48	2.07	1.12	1.57	0.4
ID 105367925	1.09	2.37	1.01	1.84	1.0
ID 105379106	1.23	1.87	1.09	1.83	1.0
Sub-Solar Sample					
ID 101121348	0.88	1.33	0.95	1.24	0.2
ID 101710670	0.83	1.33	0.90	0.74	0.02
ID 102752622	0.49	1.72	0.31	0.37	0.0003
ID 102770893	0.53	2.17	0.73	0.63	0.002

Table 1 continued on next page

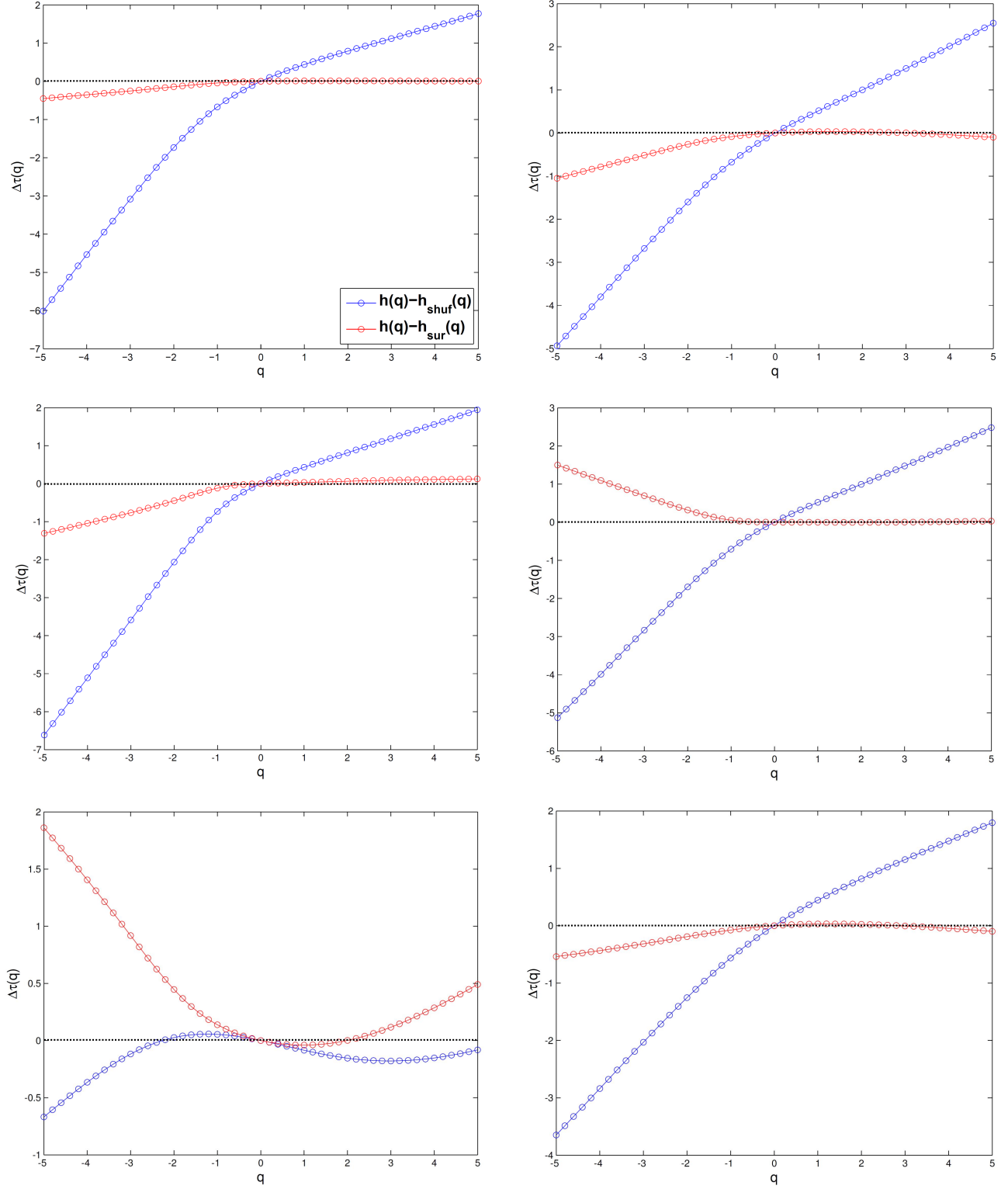


**Figure 6.** Same procedure proposed in figure 5 according to the sequence of the named stars in Figures 2, 3 and 4.

---

*Table 1 continued on next page*

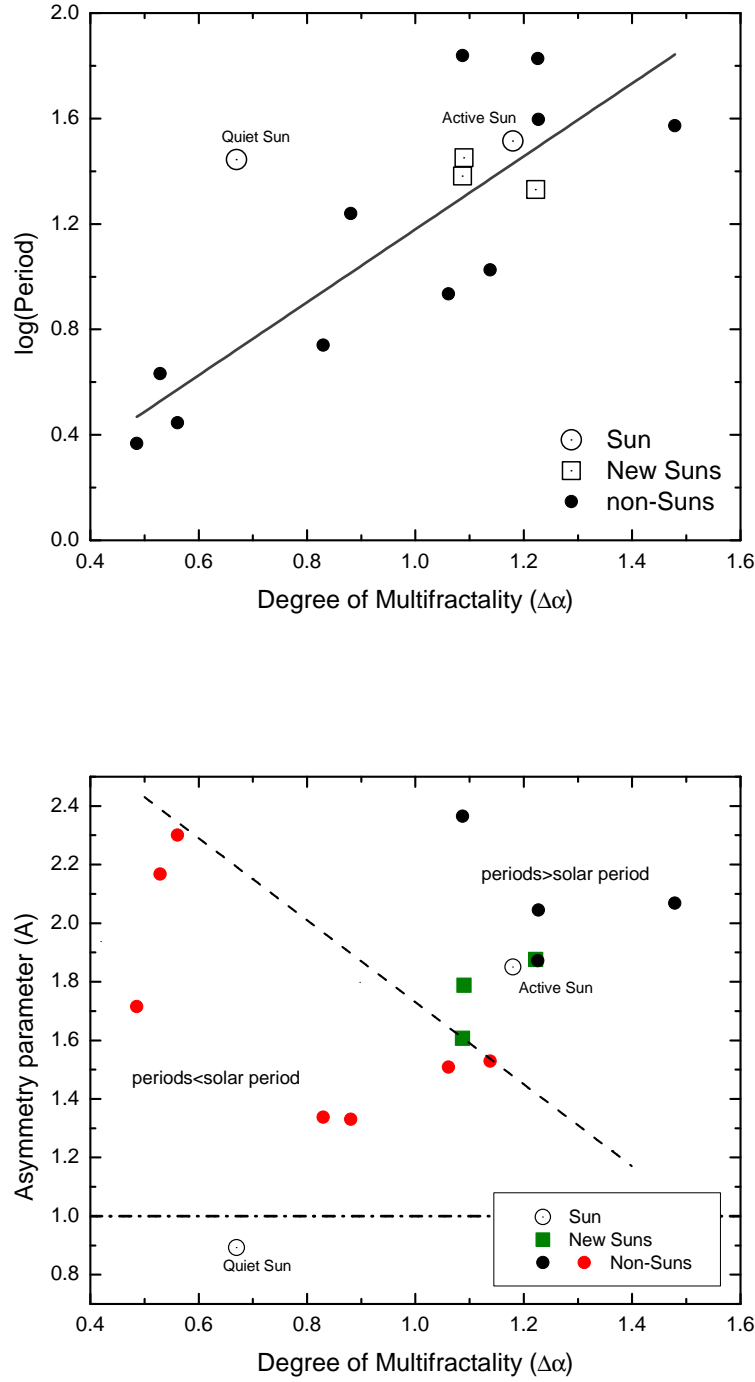


**Figure 7.** Plotted values of the degree of multifractality ( $\Delta\alpha$ ), derived on the basis of multifractal analysis, as a function of rotation period. The Sun was analyzed in its active and quiet phases. The solid line denotes the linear regression with the very similar adjustment to Equation 1 derived by [de Freitas et al. \(2013b\)](#) (top).  $\Delta\alpha$  plotted as a function of the asymmetry parameter  $A$ . The sloping line indicates the separation in two rotational regimes, while the horizontal line separate the stars in two multifractal asymmetry regimes (bottom).

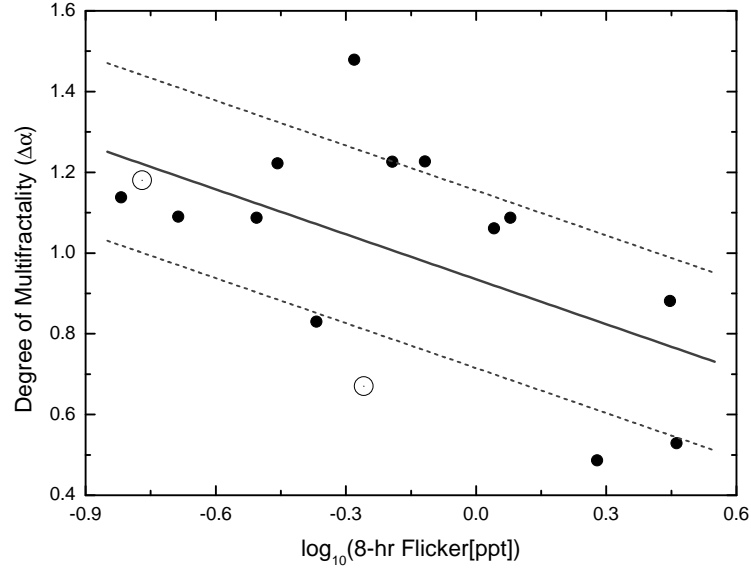


**Figure 8.** Relationship between the degree of multifractality ( $\Delta\alpha$ ) and the 8-hr flicker noise. Solid line represents the best-fitting linear regression, while short dashed lines show the 95 percent confidence level.

Table 1 (*continued*)

Star	Broadness ( $\Delta\alpha$ )	Skewness ( $A$ )	$\alpha_0$	logPer (days)	$\delta Per$ (days)
------	------------------------------	------------------	------------	------------------	------------------------

Table 1 (*continued*)

Star	Broadness ( $\Delta\alpha$ )	Skewness ( $A$ )	$\alpha_0$	logPer (days)	$\delta Per$ (days)
------	------------------------------	------------------	------------	------------------	------------------------

Table 1 (*continued*)

Star	Broadness ( $\Delta\alpha$ )	Skewness ( $A$ )	$\alpha_0$	logPer (days)	$\delta Per$ (days)
ID 105503339	1.14	1.53	0.99	1.03	0.4
ID 105945509	0.56	2.30	0.43	0.46	0.003
ID 105845539	1.06	1.51	1.02	0.94	0.4